Electronic structure of $Al_xGa_{1-x}As$-GaAs-$Al_yGa_{1-y}As$ single quantum wells subjected to in-plane magnetic fields

W. Xu

Department of Theoretical Physics, Research School of Physical Sciences and Engineering, The Australian National University, Canberra, Australian Capital Territory 0200, Australia

(Received 14 April 1994; revised manuscript received 28 November 1994)

In the presence of the high magnetic fields applied parallel to the interfaces of the $Al_xGa_{1-x}As$-GaAs-$Al_yGa_{1-y}As$ single quantum well, the electronic structure of the two-dimensional electron gas (2DEG) is calculated self-consistently at nonzero temperature. A model is developed in which the confinement potential energy, the energy and the wave function of the discrete levels, the Fermi energy, the electron density in different energy levels, and the depletion lengths can be calculated as a function of known material properties, growth parameters, and experimental conditions. The dependence of the energy and the electron density in different levels, the Fermi energy, and the depletion lengths in the selectively doped $Al_xGa_{1-x}As$ layers on the magnetic field, electron wave vector, Al content, temperature, total electron density, gate voltage, and asymmetric modulation doping is studied in detail. The experiment to measure the total electron density in a 2DEG subjected to a parallel magnetic field is discussed.

I. INTRODUCTION

A lot of published work on magnetotransport in two-dimensional electron systems (2DES's) is focused on the configuration in which the magnetic field is applied perpendicular to the interface of the 2DES. In this configuration, Landau quantization results in the important and distinctive phenomena such a Shubnikov–de Haas oscillation, quantum Hall effect, fractional quantum Hall effect, etc. The rather extensive studies[1–5] have also been made by applying the high magnetic field at an angle θ to the interface of the 2DES's. In this situation, the confinement potential (taken along the z direction) of the 2D electron gas (2DEG) and the potential caused by the tilted magnetic field lead to hybrid magnetoelectric quantization of electron energies. The study of 2D magnetotransport in this configuration has the important application to, e.g., the measurement of the enhanced spin-g factor.[6]

In this paper, we deal with a particular configuration where the magnetic field is applied parallel to the interface of the 2DES, e.g., the case of $\theta=0$. This study is essential[2] to the problem of a given arbitrary angle θ. Further, 2DEG subjected to an in-plane magnetic field shows some important and unusual behaviors such as a long period oscillation of the magnetoresistance R_{xx} with the magnetic field,[7] the oscillation and jump of the magnetization with the chemical potential,[2,4,8] vertical transport,[9] very recently the Aharonov-Bohm effect,[10] etc. The structure of the energy levels in this geometry plays an essential role in determining all the above-mentioned physical properties. In the above quoted references, the theoretical studies of the electronic structure of 2DES in parallel magnetic fields were based on taking simple analytically solvable confinement potential energies or on using the perturbative treatment. Recently, the self-consistent calculations have been proposed[11,12] in order to have a more detailed understanding of the structure. In the work of Refs. 11 and 12, the samples of $Al_xGa_{1-x}As/GaAs$ heterojunctions were taken into account. In $Al_xGa_{1-x}As/GaAs$ heterojunctions, normally only the lowest electronic subband is occupied[13] by electrons at zero magnetic field when the total electron density per unit area is less than 6×10^{16} m^{-2}. In this paper, we are interested in the samples in which more than one subbands are occupied at zero magnetic field through looking into the $Al_xGa_{1-x}As$-GaAs-$Al_yGa_{1-y}As$ single-quantum-well (SQW) systems. For a modulation-doped SQW at $B=0$, the occupancy of electrons to the electronic subbands can be easily varied by changing the width of the well layer.[14] The self-consistent calculation on the SQW subjected to in-plane magnetic fields has been made by Ref. 15, where the studies were concentrated on the quantity of capacitance. In the present paper, the self-consistent calculations proposed by Refs. 16 for the case of $B=0$ will be generated to calculate the electronic states of the SQW in parallel magnetic fields. The method of our self-consistent calculation is described in Sec. II. The experimental measurement to determine the total electron density in the present configuration is also discussed in Sec. II. In Sec. III, the numerical results are presented and discussed. The conclusions are summarized in Sec. IV.

II. OUTLINE OF THE MODEL AND THE CALCULATION

A. 2DEG in parallel magnetic fields

In the presence of a magnetic field, the free-electron Hamiltonian in a 2DES with a single-electron approximation is given by

$$H=\tfrac{1}{2}(\mathbf{p}-\mathbf{A})\frac{1}{m^*(z)}(\mathbf{p}-\mathbf{A})+U_0(z)\ , \tag{1}$$

where $\mathbf{p}=(\hat{p}_x,\hat{p}_y,\hat{p}_z)$ is the momentum operator, $\mathbf{A}$ is the

vector potential, the effective electron mass is $m^*(z)$, which is assumed to be various along the z axis, and $U_0(z)$ is the confinement potential energy along the z direction at zero magnetic field. In the presence of an in-plane magnetic field applied along the x direction $\mathbf{B}=(B_x,0,0)$, the vector potential in the Landau gauge is given by $\mathbf{A}=(0,eB_xz,0)$, and the free-electron Hamiltonian becomes

$$H=\frac{1}{2m^*(z)}\left[\hat{p}_x^2+(\hat{p}_y-eB_xz)^2+m^*(z)\hat{p}_z\frac{1}{m^*(z)}\hat{p}_z\right]+U_0(z)\ . \tag{2}$$

In Eq. (2), the momentum components p_x and p_y are constants of motion, which results in the factorized wave function of the kind $\Psi(x,y,z)=e^{i(k_xx+k_yy)}\psi_i(z)$ and in the corresponding energy spectrum of the electron $E_i(k_x,k_y)=E(k_x)+\varepsilon_i(k_y)$. When the parabolic band structure is considered, $E(k_x)=\hbar^2k_x^2/2m^*$ is the kinetic energy for free-electron motion in the x direction with m^* the representative density-of-states effective electron mass. The electron wave function $\psi_i(z)$ and the energy of the discrete level $\varepsilon_i(k_y)$ are determined by the one-dimensional Schrödinger equation

$$\left[-\frac{\hbar^2}{2}\frac{d}{dz}\frac{1}{m^*(z)}\frac{d}{dz}+U_B(z,k_y)+U_0(z)-\varepsilon_i(k_y)\right]\psi_i(z)=0\ , \tag{3}$$

where $U_B(z,k_y)=\hbar^2(k_y-z/l^2)^2/2m^*(z)$ is the potential energy induced by the in-plane magnetic field and $l=(\hbar/eB_x)^{1/2}$ is the radius of the ground cyclotron orbit.

A 2DES subjected to an in-plane magnetic field results in the quantization of electron motion along the y and z axis and provides a quasi-one-dimensional energy structure. The free-electron Green function is given by $G_{i,k_y}(E,k_x)=[E-E_i(k_x,k_y)+i\delta]^{-1}$, whose imaginary part is obtained by $\mathrm{Im}G_{i,k_y}(E,k_x)=-\pi\delta[E-E_i(k_x,k_y)]$. Thus, the density of states (DOS) for electrons in the energy level i becomes

$$D_{i,k_y}(E)=\frac{g_s}{2l}\left[-\frac{1}{\pi}\right]\sum_{k_x}\mathrm{Im}G_{i,k_y}(E,k_x)=\frac{g_s\sqrt{2m^*}}{4\pi\hbar l}\frac{\Theta[E-\varepsilon_i(k_y)]}{\sqrt{E-\varepsilon_i(k_y)}}\ , \tag{4}$$

where $\Theta(x)=0(x<0)$, $1(x\geq 0)$ is the unit-step function, g_s is the factor for spin degeneracy, and the degeneracy of each energy level is $1/2l$ per unit length. We note that in the absence of the z-direction confinement potential energy $U_0(z)$, the degeneracy of each Landau level in the yz plane is given by $1/2\pi l^2$ per unit area. The presence of $U_0(z)$ lifts the z direction degeneracy.

B. Modulation-doped $Al_xGa_{1-x}As$-GaAs-$Al_yGa_{1-y}As$ single quantum wells

In general, the selectively doped $Al_cGa_{1-c}As$-GaAs-$Al_cGa_{1-c}As$ (with c being the aluminum content) SQW systems can be depicted in Fig. 1.

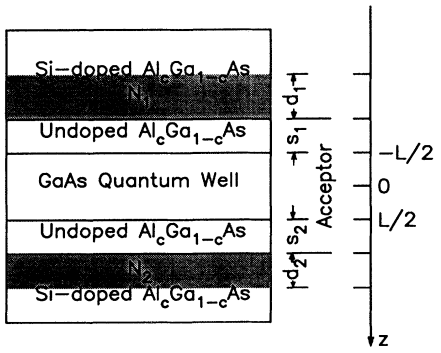

FIG. 1. Schematic diagram of a modulation-doped $Al_cGa_{1-c}As$-GaAs-$Al_cGa_{1-c}As$ single quantum well. c is the aluminum content. L is the width of the quantum well. d_j, N_j, and s_j $(j=1, 2)$ are the depletion length, modulation-doped donor concentration, and spacer distance in the jth $Al_xGa_{1-x}As$ layer, respectively.

(1) A SQW consists of a GaAs well layer (with a width L) adjacent to two $Al_cGa_{1-c}As$ barrier layers. The $Al_xGa_{1-x}As$ layers are uniformly doped with Si with the concentrations N_1 and N_2 except for the (spacer) layers of widths s_1 and s_2, respectively, measured from the interfaces between GaAs and $Al_xGa_{1-x}As$. The GaAs layer along with the Si-undoped $Al_xGa_{1-x}As$ spacer layers are slightly and uniformly doped with acceptors with the concentration N_a.

(2) The modulation-doped Si in $Al_xGa_{1-x}As$ layers will play a role of donors, which are not completely ionized because of the depletion effect. We assume that the doped Si are only ionized within the (shaded) regimes $-d_1-s_1-L/2<z<-s_1-L/2$ and $L/2+s_2<z<L/2+s_2+d_2$, respectively. The depletion lengths d_1 and d_2 can be determined by the self-consistent calculations.

(3) For a sample without heavy acceptor doping and with a relatively thin GaAs layer, we may assume that all the acceptors are ionized. For a high-quality sample, the acceptor concentration is very small compared with doped donor concentration; we may neglect the influence of acceptors in Si-doped $Al_xGa_{1-x}As$ regimes.

(4) In equilibrium state, the Fermi energy (or chemical potential) E_F is a constant across the sample system due to thermodynamic equilibrium.

Our present calculation on the SQW systems goes beyond the previous work[17] through considering the effect of asymmetric modulation doping, i.e., possibly $s_1\neq s_2$ and/or $N_1\neq N_2$. The asymmetric-doped SQW structure exhibited some unusual transport phenomena observed experimentally.[18]

For selectively doped $Al_cGa_{1-c}As$-GaAs-$Al_cGa_{1-c}As$ SQW systems, the effective electron-mass ratio can be obtained by[19]

$$\frac{m^*(z)}{m_e}=\begin{cases}m_0^*/m_e, & |z|<L/2\\ m_0^*/m_e+0.088c & \text{otherwise}\ ,\end{cases} \tag{5}$$

with m_e the electron rest mass and m_0^* the effective elec-

tron mass for GaAs, i.e., for $c=0$; the confinement potential energy at zero magnetic field in Eq. (3) is given by

$$U_0(z)=U_c(z)+U_{xc}(z)+\Delta E_c(z) , \quad (6)$$

where $\Delta E_c(z)$ is the conduction-band-edge discontinuity, in the well (i.e., in GaAs) $\Delta E_c(z)=0$ and in the barrier (i.e., in $Al_cGa_{1-c}As$) $\Delta E_c(z)=U_0$, which can be determined by[19]

$$U_0 \simeq 0.6(1.155c+0.37c^2) \ (\text{eV}) . \quad (7)$$

Further, the potential energy $U_{xc}(z)$ results from the exchange-correlation effects in the density-functional theory (DFT); the potential energy $U_c(z)$ is the Coulomb interaction term arising from charge interaction and can be determined by the Poisson equation

$$\frac{d}{dz}\kappa(z)\frac{d}{dz}U_c(z)=e\rho(z) , \quad (8)$$

where $\rho(z)$ and $\kappa(z)$ are the charge distribution and the dielectric constant along the z direction, respectively. In this paper, we ignore the difference of the dielectric constant in GaAs and $Al_xGa_{1-x}As$ because of the relatively weak effect.[17] We assume an isotropic κ in the sample system, i.e., $\kappa(z)\simeq\kappa$.

In general the exchange-correlation potential energy is an unknown functional $U_{xc}(z)=U_{xc}[n(z)]$ of the electron density $n(z)$. For a 2DEG in strong perpendicular magnetic fields, the magnetic exchange energy in the low temperature limit $T\rightarrow 0$ has been calculated by several authors.[20,21] The study of Ref. 21 shows that the difference between the $B=0$ and $B\neq 0$ exchange energies is through the coefficients regarding the first- and second-order exchange contributions, the second-order direct contribution, and through the parameter r_s; for the systems with completely filled Landau levels, at high electron densities and strong magnetic fields, the total energy is lowered by the magnetic field. However, the numerical results presented in Fig. 2 of Ref. 21 show only a slight difference in the total energies obtained with and without magnetic field. As a result, the kinetic energy will not be changed by the magnetic field. Furthermore, we notice that the coefficients regarding the exchange-energy parts, shown in Table I of Ref. 21, depend weakly on the magnetic field. For example, the first-order exchange contribution is essential for the lowering of the exchange energy by magnetic field. The corresponding coefficient c_m varies very little, from 1.70 at $B=0$–1.77 at a magnetic field strong enough that only the lowest Landau level is occupied. For a 2DEG subjected to a parallel magnetic field, the magnetic effect is included in the confinement potential energy in the z direction [see Eq. (3)], which affects r_s only through $n(z)$. In this case, we expect an even *weaker* dependence of the exchange-correlation effect on the magnetic field in comparison with the case in the presence of perpendicular magnetic fields.

The brief discussion given above indicates that the results obtained from the zero-magnetic-field calculation of the exchange-correlation energy may be applied to the situation in the presence of a parallel magnetic field. In this paper, we employ an analytic form (obtained at zero-magnetic-field limit) to evaluate the exchange-correlation potential energy over a wide range of temperatures and electron densities through[22]

$$U_{xc}(z)=U^0_{xc}[n(z)]\begin{cases}1, & \gamma\leq 0.15\\ 1+(a_1r_s^2+b_1r_s+c_1)\gamma^e/(a_1^*r_s+b_1^*+\gamma^d), & 0.15<\gamma\leq 12 ,\end{cases} \quad (9a)$$

where $\gamma=k_BT/E_F$, $a_1=-0.003\,88$, $b_1=0.045\,44$, $c_1=-0.443$, $a_1^*=1.5460$, $b_1^*=0.7023$, $e=2.042\,58$, $d=1.805\,18$, and $r_s=r_s[n(z)]=[4\pi a^{*3}n(z)/3]^{-1/3}$ with the effective Bohr radius $a^*=4\pi\kappa\hbar^2/[e^2m^*(z)]$. We use the result for exchange-correlation potential energy at $T\rightarrow 0$ through[23]

$$U^0_{xc}[n(z)]=-[1+0.7734y\ln(1+y^{-1})]\frac{2R_y^*}{\pi\alpha r_s} , \quad (9b)$$

where $\alpha=(4/9\pi)^{1/3}$, $y=y(z)=r_s/21$, and the effective Rydberg constant is given by $R_y^*=e^2/(8\pi\kappa a^*)$. In $Al_xGa_{1-x}As$-GaAs-$Al_yGa_{1-y}As$ SQW structures, the potential energy $U_{xc}(z)$ may be discontinuous at the interfaces between GaAs and $Al_xGa_{1-x}As$ (i.e., at $z=\pm L/2$) because of different effective electron masses.

For an $Al_xGa_{1-x}As$-GaAs-$Al_yGa_{1-y}As$ SQW depicted by Fig. 1, the functional form of the charge density $\rho(z)$ can be modeled by

$$\rho(z)=-e\begin{cases}n(z), & z<d_1-s_1-L/2\\ n(z)-N_1, & -d_1-s_1-L/2<z<-s_1-L/2\\ n(z)+N_a, & -s_1-L/2<z<L/2+s_2\\ n(z)-N_2, & L/2+s_2<z<L/2+s_2+d_2\\ n(z), & z>L/2+s_2+d_2 ,\end{cases} \quad (10)$$

where the electron density along the z direction is given by

$$n(z)=\sum_{i,k_y}|\psi_i(z)|^2\int_{-\infty}^{\infty}dE\,f(E)D_{i,k_y}(E)$$
$$=\frac{\sqrt{2m_0^*}}{2\pi\hbar l}\sum_{i,k_y}|\psi_i(z)|^2\int_0^{\infty}\frac{dE}{\sqrt{E}}f[E+\varepsilon_i(k_y)] , \quad (11)$$

with $f(E)=[e^{(E-E_F)/k_BT}+1]^{-1}$ the Fermi-Dirac func-

tion. The Fermi energy can be determined by the condition of the electron number conservation $n_T=\sum_i n_i$ with n_T the total electron density per unit area and the electron density in the energy level i

$$n_i=\sum_{k_y}\int_{-\infty}^{\infty} dE\, f(E)D_{i,k_y}(E)$$
$$=\frac{\sqrt{2m_0^*}}{2\pi\hbar l}\sum_{k_y}\int_0^{\infty}\frac{dE}{\sqrt{E}}f[E+\varepsilon_i(k_y)]\ . \tag{12}$$

In Eqs. (11) and (12), we have used (i) the DOS shown in Eq. (4), and (ii) the effective electron mass in the well layer as the representative density-of-states effective mass, i.e., $m^*=m_0^*$, and we have taken $g_s=2$.

To solve Eq. (8) with the charge distribution given by Eq. (10), we need to define the boundary conditions. The nature of $\psi_i(\pm\infty)=0$ results in $n(\pm\infty)=0$, $U_{xc}(\pm\infty)=0$, $\rho(\pm\infty)=0$, and consequently in $dU_0(z)/dz|_{z\to\pm\infty}=0$. Thus, we can integrate both Schrödinger and Poisson equations from $-\infty$ to $+\infty$ along the z axis. In this paper, we choose the zero of energy as $U_0(-\infty)=0$, and in the presence of a gate voltage V_g applied along the z axis, we have $U_0(+\infty)=V_g$. After (i) assuming $\kappa(z)\simeq\kappa$, (ii) using the above boundary conditions, (iii) using the continuities of $U_c(z)$ and $dU_c(z)/dz$ in the z direction, and (iv) integrating Eq. (8) twice, we obtain

$$U_c(z)=\begin{cases} U_L(z), & z\le -d_1-s_1-L/2 \\ U_L(z)-DN_1(z+d_1+s_1+L/2)^2, & -d_1-s_1-L/2\le z\le -L/2-s_1 \\ U_L(z)-DN_1d_1(d_1+L+2s_1+2z)+DN_a(L/2+s_1+z)^2, & -L/2-s_1\le z\le 0 \\ U_R(z)-DN_2d_2(d_2+L+2s_2-2z)+DN_a(L/2+s_2-z)^2, & 0\le z\le L/2+s_2 \\ U_R(z)-DN_2(z-d_2-s_2-L/2)^2, & L/2+s_2\le z\le L/2+s_2+d_2 \\ U_R(z), & z\ge L/2+s_2+d_2\ , \end{cases} \tag{13}$$

where $D=-e^2/2\kappa$, $U_L(z)=2Dg(z)-U_0$, and $U_R(z)=2Dh(z)-U_0+V_g$ are the potential energies induced by electron distribution, i.e., $d^2U_L(z)/dz^2=d^2U_R(z)/dz^2=2Dn(z)$, and $g(z)$ and $h(z)$ are given, respectively, by

$$g(z)=\int_{-\infty}^{z}dz_1\int_{-\infty}^{z_1}dz_2 n(z_2)$$
$$h(z)=\int_{+\infty}^{z}dz_1\int_{+\infty}^{z_1}dz_2 n(z_2)\ .$$

The continuities of $dU_c(z)/dz$ and $U_c(z)$ at $z=0$ lead to, respectively,

$$n_T=\int_{-\infty}^{\infty}dz\, n(z)=N_1d_1+N_2d_2-N_a(L+s_1+s_2)\ , \tag{14a}$$

which can also be obtained from the charge-neutrality condition, and

$$N_1d_1(d_1+L+2s_1)-N_2d_2(d_2+L+2s_2)$$
$$=N_a(s_1-s_2)(L+s_1+s_2)+2\left[g(0)-h(0)-\frac{V_g}{2D}\right]\ . \tag{14b}$$

At $V_g=0$ and for symmetric modulation doping, i.e., for $s_1=s_2$ and $N_1=N_2$, Eq. (14b) leads to $d_1=d_2$. Generally, $d_1\neq d_2$ for asymmetric doping and/or in the presence of the gate voltage. By solving Eqs. (14), we can determine the depletion lengths d_1 and d_2, which make $dU_c(z)/dz$ and $U_c(z)$ continuous along the z direction. When the solutions satisfy $d_j>0$ $(j=1,2)$, some donors are ionized in the jth $Al_xGa_{1-x}As$ layer. When $d_j<0$, some electrons are accumulated in the jth $Al_xGa_{1-x}As$ layer; in this situation, parallel conduction may occur.

C. Self-consistent calculation on the electronic structure

In this paper, we use an iteration technique to solve Schrödinger equation for the eigenfunction and eigenvalue, and Poisson equation for the confinement potential self-consistently. First, applying the turning-point technique to the Numerov algorithm,[24] the Schrödinger equation can be solved by using the boundary conditions $\psi_i(\pm\infty)=0$. Second, the wave function and the energy of the electronic levels are used to determine the Fermi energy E_F [Eq. (12)], the electron distribution $n(z)$ [Eq. (11)], the exchange-correlation potential energy [Eq. (9)], $g(z)$, and $h(z)$. Then, the depletion lengths d_1 and d_2 can be calculated by using Eq. (14). Introducing the results of the depletion lengths as well as $g(z)$ and $h(z)$ into Eq. (13), we can calculate the Hartree potential energy $U_c(z)$. Thus, we obtain for the total confinement potential energy $U(z)=U_B(z,k_y)+U_0(z)$. In the self-consistent calculations, the iteration is interrupted when $\max|U_{j+1}(z)-U_j(z)|$, i.e., the maximum difference of the total confinement potential energy between two successive iteration steps j and $j+1$, is smaller than 0.1 meV.

The inputs of the self-consistent calculation are (1) known material properties, such as effective electron mass for GaAs (m_0^*) and dielectric constant of the material of GaAs (κ); (2) sample growth parameters, such as concentrations of acceptors (N_a) and modulation-doped donors (N_1 and N_2), spacer distances (s_1 and s_2), thickness of the GaAs well layer, and Al content (c); (3) experimental conditions, such as magnetic field (B_x), tempera-

ture (T), and gate voltage (V_g); and (4) results of the electron wave vector (k_y) and the total electron density per unit area (n_T). As outputs, our self-consistent calculations will give (1) the total confinement potential energy; (2) the energy and the wave function for the electronic states; (3) the electron distribution function along the direction perpendicular to the interfaces of the quantum well; (4) the depletion lengths; (5) the Fermi energy; and (6) the electron density in different energy levels.

In general, k_y is a good quantum number resulting from the gauge choice. The determination of the range over which k_y is defined is very complicated and CPU time consuming in the self-consistent calculation. A proposed way[11] to determine k_y is by using the Fermi contours $E_i(k_x,k_y)\leq E_F$. However, this technique can only be applied to the situation of zero temperature and noninteracting (i.e., no scattering) electrons, otherwise, the new contours have to be introduced. Fortunately, the numerical results obtained from the present calculation show that (see Fig. 3) in the single-quantum-well structures, although the actual value of k_y does affect the shape of the total confinement potential, the difference between the energy levels *below* the Fermi energy and the Fermi energy is constant over a wide range of k_y. The results are that the total electron density and the electron density in the occupied subbands are constant with varying k_y, which implies that the quantum number k_y can be taken as a *quasifree* parameter for the SQW systems. Hence, the numerical calculation can be simplified greatly. The detailed discussion on this point is presented in Sec. III. In this paper, we are interested in the solution of the Schrödinger equation and Poisson equation along the z direction and take k_y as an input parameter. Since the potential energy is constant in the y direction, k_y is not affected by this self-consistent procedure. The total electron density n_T can be obtained from the experimental measurements, which will be discussed in the next subsection.

D. The determination of the total electron density

In the presence of an in-plane magnetic field, the total confinement potential energy of a 2DES along the z axis will be varied. Additionally, the DOS in this configuration differs from that at $B_x=0$. They may lead to the different electron energy levels and the Fermi energy. Consequently, the total electron density at $B_x\neq 0$ may differ from that in case of $B_x=0$. For a 2DEG subjected to an in-plane magnetic field, the total electron density per unit area can still be measured in the Hall configuration,[25] where an additional magnetic field B_z applied along the z direction is present. However, due to the cyclotron motion of electrons in the yz plane, caused by B_x, the total electron density cannot be determined simply by the conventional Hall measurement.

A simple Drude model can be employed to study the electron transport in crossed electric and magnetic fields. Under the relaxation-time approximation,the equation of motion of an electron is given by $m^*(O+1/\tau)\mathbf{v}=-e\mathbf{F}=-e(\mathbf{E}+\mathbf{v}\times\mathbf{B})$, where $O=d/dt$, τ is the relaxation time induced by the electron scattering mechanisms, and $\mathbf{v}=[v_x(t),v_y(t),v_z(t)]$ is the average electron velocity at time t. For the case $\mathbf{E}=(E,0,0)$ and $\mathbf{B}=\mathbf{B}_1+\mathbf{B}_2$ with $\mathbf{B}_1=(B_x,0,0)$ and $\mathbf{B}_2=(0,0,B_z)$, we have

$$\begin{aligned}(O+1/\tau)v_x(t)&=-\omega_z[E/B_z+v_y(t)]\ ,\\ (O+1/\tau)v_y(t)&=-\omega_z[\omega_x v_z(t)/\omega_z-v_x(t)]\ ,\\ (O+1/\tau)v_z(t)&=\omega_x v_y(t)\ ,\end{aligned}\tag{15}$$

with $\omega_x=eB_x/m^*$ and $\omega_z=eB_z/m^*$ being the cyclotron frequencies. The solution of Eq. (15) is obtained by

$$\begin{aligned}v_x(t)&=v_x+e^{-t/\tau}[c_1-(c_2\sin\omega_0 t-c_3\cos\omega_0 t)\omega_z/\omega_0]\ ,\\ v_y(t)&=v_y+e^{-t/\tau}(c_2\cos\omega_0 t+c_3\sin\omega_0 t)\ ,\\ v_z(t)&=v_z+e^{-t/\tau}[c_4+(c_2\sin\omega_0 t-c_3\cos\omega_0 t)\omega_x/\omega_0]\ ,\end{aligned}\tag{16}$$

where $\omega_0=\sqrt{\omega_x^2+\omega_z^2}$; c_1, c_2, c_3, and c_4 are the integration constants, which can be determined by the initial conditions; the steady-state solution of Eq. (15) is obtained by, after taking $t\rightarrow\infty$ in Eq. (16),

$$\begin{aligned}v_x&=-(E/B_z)(\omega_z\tau)[1+(\omega_x\tau)^2]/[1+(\omega_0\tau)^2]\ ,\\ v_y&=-(E/B_z)(\omega_z\tau)^2/[1+(\omega_0\tau)^2]\ ,\\ v_z&=-(E/B_z)(\omega_x\omega_z^2\tau^3)/[1+(\omega_0\tau)^2]\ .\end{aligned}\tag{17}$$

Using the Onsager relationship for 2DEG in the linear response regime, the magnetoresistivities for a 2DEG subjected to electric (E) and magnetic (B_x and B_z) fields is obtained by

$$\begin{aligned}\rho_{xx}&=\frac{E}{n_T e}\frac{|v_x|}{v_x^2+v_y^2}\\ &=\frac{m^*}{n_T e^2\tau}\left[1+\frac{\omega_x^2\omega_z^2\tau^4}{1+2(\omega_x\tau)^2+(\omega_z\tau)^2+(\omega_x\tau)^4}\right]\end{aligned}\tag{18a}$$

and

$$\begin{aligned}\rho_{xy}&=\frac{E}{n_T e}\frac{|v_y|}{v_x^2+v_y^2}\\ &=\frac{B_z}{n_T e}\frac{1+(\omega_x^2+\omega_z^2)\tau^2}{1+2(\omega_x\tau)^2+(\omega_z\tau)^2+(\omega_x\tau)^4}\ .\end{aligned}\tag{18b}$$

Here one finds that the total electron density can only be simply measured by $\rho_{xy}=B_z/n_T e$ (conventional Hall effect) in case of $B_x=0$, i.e., $\omega_x=0$. For strong parallel (B_x) and weak perpendicular (B_z) magnetic fields so that $\omega_x^2\gg\omega_z^2$, we have

$$\rho_{xx}\simeq\frac{m^*}{n_T e^2\tau}\quad\text{and}\quad\rho_{xy}\simeq\frac{B_z}{n_T e}\frac{1}{1+(\omega_x\tau)^2}\ .\tag{19}$$

Noting $\omega_x\tau=B_x\mu$ with $\mu=e\tau/m^*$ the electron mobility for the corresponding sample structure and applied fields, the total electron density for a high mobility sample, so that $(B_x\mu)^2\gg 1$ is satisfied, can be obtained from measuring both ρ_{xx} and ρ_{xy}

$$n_T\simeq e\frac{\rho_{xy}B_x^2}{\rho_{xx}^2 B_z}\ .\tag{20}$$

The experimental work to study the influence of parallel magnetic field on the total electron density in 2DES has not yet been reported.

III. NUMERICAL RESULTS AND DISCUSSIONS

In this paper, our calculations are performed for $Al_xGa_{1-x}As$-GaAs-$Al_yGa_{1-y}As$ single quantum wells by taking the material parameters: (i) the effective mass of GaAs $m_0^*=0.0665m_e$ and (ii) the dielectric constant of GaAs $\kappa=12.9$. The growth parameters can be taken from the experimental data.

The numerical results of the total confinement potential energy and the electron density as function of the distance along the z direction of a SQW are shown in Fig. 2 for fixed width of quantum well and the total electron density in the presence (solid curves) and absence (dotted curve for comparison) of the parallel magnetic field. The results for $B_x=0$ are obtained by applying the DOS for 2DEG $D_i(E)=(m_0^*/\pi\hbar^2)\Theta(E-\varepsilon_i)$ to the above presented formulas and by taking $U_B(z,k_y)=0$. In Fig. 2, the energy of the different electronic subband ε_i are also shown for the cases of $B_x\neq 0$ and $B_x=0$. The presence of the parallel magnetic field will lead to an extra parabolic type of confinement potential energy along the z direction. Since we have taken $k_y=0$, $V_g=0$, and symmetric modulation doping ($s_1=s_2$ and $N_1=N_2$), the total confinement potential energies in Fig. 2 show the symmetric nature. In Fig. 2(b), different electron distributions can be found in cases with and without magnetic field B_x, which results from the different electron densities in the occupied levels (see caption of Fig. 2). The results obtained from the self-consistent calculation show that the presence of the parallel magnetic field leads to very little variation of the depletion lengths in the $Al_xGa_{1-x}As$ layers.

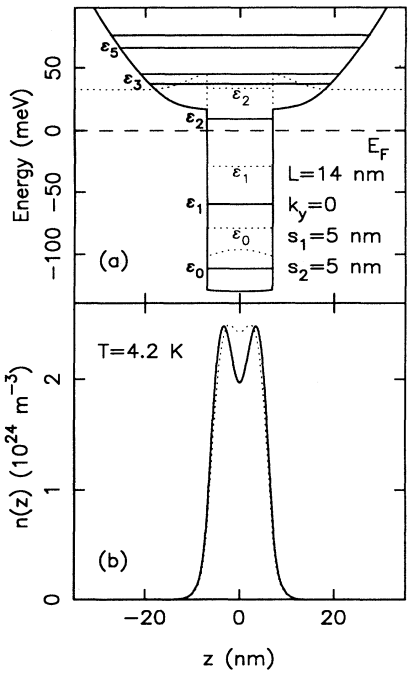

FIG. 2. (a) The confinement potential energy and (b) the electron distribution along the direction perpendicular to the interfaces of an $Al_{0.2}Ga_{0.8}As$-GaAs-$Al_{0.2}Ga_{0.8}As$ SQW in the presence (solid curves, $B=10$ T) and absence (dotted curves) of the parallel magnetic field for the fixed width of quantum well $L=14$ nm, spacers $s_1=s_2=5$ nm, modulation-doped donor concentrations $N_1=N_2=2\times10^{24}$ m^{-3}, background acceptor density $N_a=8\times10^{20}$ m^{-3}, total electron density $n_T=3\times10^{16}$ m^{-2}, temperature $T=4.2$ K, electron wave vector $k_y=0$, and gate voltage $V_g=0$. E_F is the Fermi energy. In (a), ε_i is the energy for the ith level. The electron density in the occupied levels for $B=10$ T ($B=0$) are $n_0=1.73\times10^{16}$ m^{-2} ($n_0=2.20\times10^{16}$ m^{-2}); $n_1=1.27\times10^{16}$ m^{-2} ($n_1=8.0\times10^{15}$ m^{-2}). The depletion lengths are $d_1=d_2=7.51$ nm both for $B=10$ T and $B=0$.

The importance of electron wave vector k_y to the electronic subband structure of 2DES's in in-plane magnetic fields has been noticed by Refs. 2, 4, 11, and 12. To check if the issue (or argument) used in the present self-consistent calculation is right or not, i.e., whether or not k_y can be taken as a quasifree parameter for SQW's, the influence of k_y on energy level, Fermi energy, and electron density in different states in a SQW is shown in Fig. 3 for a fixed in-plane magnetic field. Our numerical results show that (1) the electron density in the occupied energy levels depends very little on k_y [see Fig. 3(b)]; (2) the parabolic nature can be found for the occupied energy levels $\varepsilon_i<E_F$ and for the Fermi level; (3) the difference between the energy of the occupied levels and the Fermi energy is constant with varying k_y; and (4) the oscillation with k_y can be found for unoccupied levels. The oscilla-

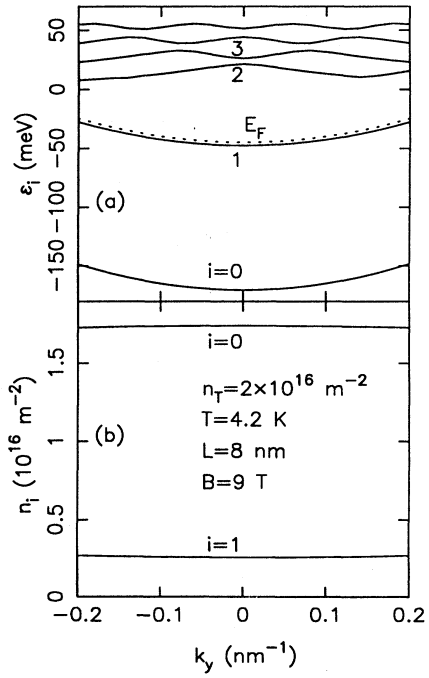

FIG. 3. (a) ε_i, E_F, and (b) n_i as a function of the electron wave vector for an $Al_{0.3}Ga_{0.7}As$-GaAs-$Al_{0.3}Ga_{0.7}As$ SQW at $V_g=0$. The sample parameters such as N_j, s_j ($j=1,2$) and N_a are the same as in Fig. 2.

tion of the energy levels with the parallel magnetic field was also observed by Refs. 2 and 4. The most significant conclusion we draw from Fig. 3 is that the actually measurable properties such as electron density and the subband energy referred to the Fermi energy are almost independent on the value of k_y over a wide range of choosing k_y. We note that at magnetic field $B_x=9$ T, the center of the cyclotron orbits $Z=l^2k_y$ moves along the z direction in the range $-15<Z<15$ nm when k_y varies from -0.2 to 0.2 nm^{-1}. This is much larger than the regime $-4<z<4$ where the electrons are most probably located in. The physical reason that results in a weak influence of quantum number k_y on the electronic properties in a SQW sample is that (i) when $|Z|<L/2$ (small k_y case) the influence of B_x on the total confinement potential energy is small. At $B_x=9$ T and $|Z|\leq L/2$ with $L=8$ nm, $\max[U_B(z,k_y)]<0.8$ meV is much smaller than the confinement potential energy U_0 ($U_0=227$ meV for an $Al_{0.3}Ga_{0.7}As$-GaAs-$Al_{0.3}Ga_{0.7}As$ SQW sample); and (ii) when $|Z|>L/2$ (large k_y case), the center of the parabolic magnetic-potential $U_B(z,k_y)$ is outside the quantum-well layer and the magnetic field tends to displace the electrons away from the quantum well. Since the confinement potential energy U_0 is very large, the effects of the magnetic field are suppressed. It is necessary to point out that one cannot take k_y as a free parameter for $Al_xGa_{1-x}As/GaAs$ heterojunctions (see Figs. 1 and 2 in Ref. 11).

In the following, we discuss the dependence of the electron density and the energy of electronic subband on the sample parameters and on the experimental conditions in SQW samples. Since these electronic properties depend very little on k_y, we take $k_y=0$ as an input in the calculations and the summation over k_y in Eqs. (11) and (12) can be removed.

In Fig. 4, the energy of electronic subband, the Fermi energy, and the electron density in different levels are plotted as a function of an in-plane magnetic field. Increasing the magnetic field leads to the decrease in Fermi energy and, consequently, to the fact that the higher index energy levels are depopulated in high magnetic fields. It can be seen from Fig. 4 that the quantum-resonance effect, which occurs each time when Fermi energy passes through an energy level, can be observed by changing the parallel magnetic field. When the quantum resonance occurs, the scattering channel in an energy level opens up (or closes down), and the resonant scattering will lead to the enhancement (or suppression) of the magnetoresistance R_{xx}. This resonance effect differs from the Shubnikov–de Haas (SdH) oscillation through (1) applying a parallel magnetic field; (2) a not strongly oscillated Fermi energy with magnetic field; (3) different DOS for electrons; and (4) the resonant scattering may occur between the energy levels created mainly by the confinement at $B_x=0$ in contrast with the resonant scattering between different Landau levels for SdH oscillation. Our results can be used to interpret the experimental observation of the long period oscillation[7] of R_{xx} with the in-plane magnetic field.

In Fig. 5, we plot the energy level, the Fermi energy,

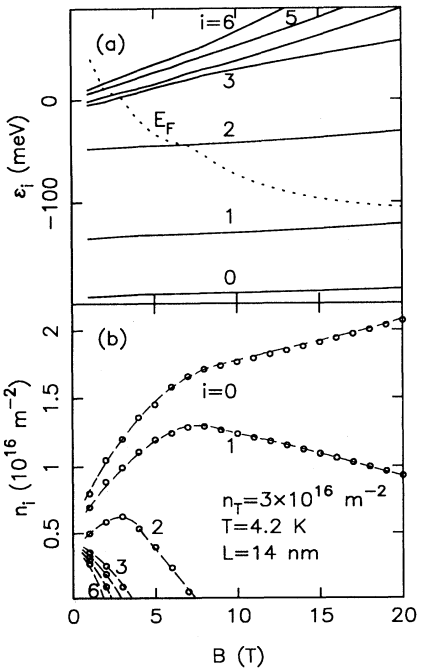

FIG. 4. (a) ε_i, E_F, and (b) n_i as a function of an in-plane magnetic field for an $Al_{0.3}Ga_{0.7}As$-GaAs-$Al_{0.3}Ga_{0.7}As$ SQW. The rest parameters are the same as in Fig. 2. In (b), the symbols are connected by the dashed curves to guide the eye.

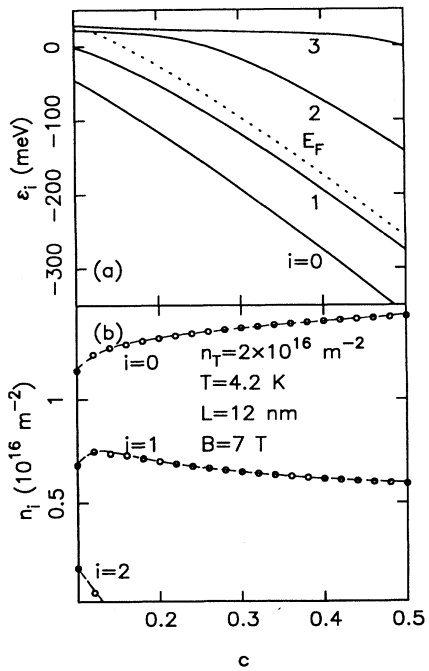

FIG. 5. The dependence of the electronic properties for an $Al_cGa_{1-c}As$-GaAs-$Al_cGa_{1-c}As$ SQW on Al content c for $V_g=0$. The conduction-band-edge discontinuity and the effective electron mass in $Al_xGa_{1-x}As$ layers are calculated by using Eqs. (7) and (5), respectively. N_j, s_j, and N_a are the same as in Fig. 2.

and the electron density in different levels as a function of Al content for $Al_cGa_{1-c}As$-GaAs-$Al_cGa_{1-c}As$ SQW's in a fixed parallel magnetic field. The stronger effect of the magnetic field can be observed for smaller values of c because the potential energy induced by the magnetic field now is comparable with the confinement potential energy caused mainly by the band discontinuity U_0 [see Eq. (7)]. The temperature dependence of the electronic properties of a SQW subjected to an in-plane magnetic field is presented in Fig. 6. The results obtained from the self-consistent calculation show that the electron density in the occupied (unoccupied) levels depends weakly on (increases rapidly with) temperature when the total electron density is fixed. Since the total electron density in SQW systems is usually high, the nonzero temperature correction of the exchange-correlation energy through Eq. (9a) is found to be small.

Experimentally, the total electron density in an $Al_xGa_{1-x}As/GaAs$ structure can be varied by, e.g., illuminations.[13] In Fig. 7, the electronic energy levels, the Fermi energy, the electron density in different levels, and the depletion lengths are plotted as function of total electron density for fixed well width and in-plane magnetic field. The rapid increase in E_F with n_T leads to the occupation of electrons to the higher energy levels and to the increase in the electron density in the occupied levels. We note that the depletion lengths increase with increasing n_T, which implies more donors in $Al_xGa_{1-x}As$ layers are ionized. The results presented in Fig. 7 indicate that the quantum-resonance effect for a SQW subjected to an in-plane magnetic field can also be observed by varying the total electron density through persistent photoconduction process. Another popular way used experimentally to vary the electronic properties of the 2DES's is through applying a gate voltage. The influence of a gate voltage on the energy levels, Fermi energy, electron densities, and depletion lengths for a SQW in the presence of a parallel magnetic field is presented in Fig. 8. With varying gate voltage V_g (1) the energy levels [see 8(a)] oscillate with V_g; (2) the occupation of electrons to the higher level can be achieved by applying a higher $|V_g|$; and (3) the depletion length in $Al_xGa_{1-x}As$ layer 1 (2) increases (decreases) with increasing V_g. $d_1=d_2$ for $V_g=0$ and for symmetric modulation doping. For a large enough gate voltage, we found the depletion length d_j may become negative. $d_j<0$ indicates that in the jth $Al_xGa_{1-x}As$ layer (see Fig. 1), (i) the doped donors are not ionized at all; (ii) the electrons are accumulated in the $As_xGa_{1-x}As$ layer; and (iii) the accumulation of electrons in the $Al_xGa_{1-x}As$ layer will result in conduction in the layer under the action of the electric field applied along the x direction. Our results for asymmetric modulation-doped SQW are shown in Fig. 9 where ε_i, E_F, n_i, and d_j ($j=1,2$) are plotted as function of spacer distance s_2 for fixed spacer $s_1=5$ nm and concentrations of modulation-doped donors $N_1=3\times10^{24}$ m^{-3} and $N_2=10^{24}$ m^{-3} in different $Al_xGa_{1-x}As$ layers shown in Fig. 1. The asymmetric modulation doping in a SQW has a weak effect on the electron density in the occupied energy levels but affects markedly the depletion length in different $Al_xGa_{1-x}As$ layers.

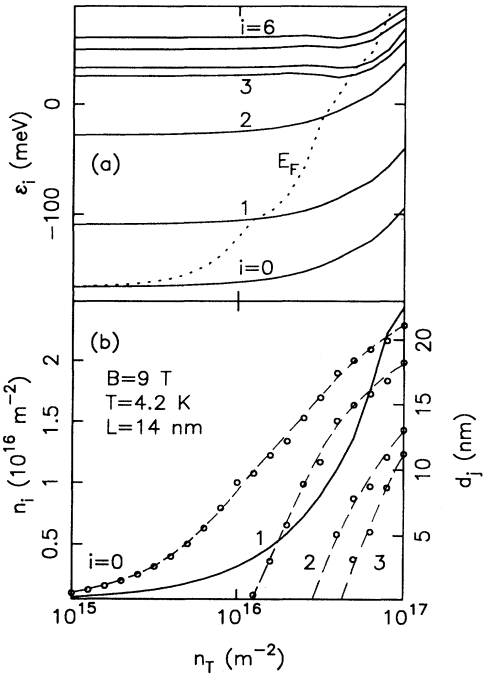

FIG. 7. (a) ε_i and E_F; (b) n_i (symbols connected by the dashed curves) and d_j (solid curve, depletion length in the jth $Al_xGa_{1-x}As$ layer) as a function of the total electron density for an $Al_{0.25}Ga_{0.75}As$-GaAs-$Al_{0.25}Ga_{0.75}As$ SQW. N_j, s_j, and N_a are the same as in Fig. 2. $d_1=d_2$ because of symmetric modulation doping and $V_g=0$.

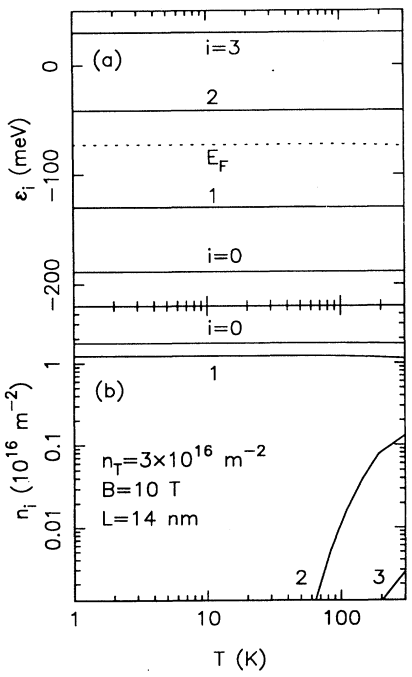

FIG. 6. Temperature dependence of electronic properties in an $Al_{0.3}Ga_{0.7}Al$-GaAs-$Al_{0.3}Ga_{0.7}As$ SQW at $V_g=0$. N_j, s_j, and N_a are the same as in Fig. 2.

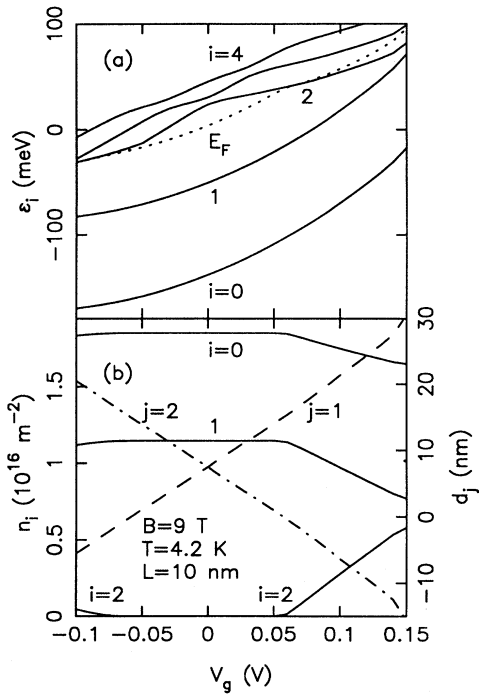

FIG. 8. (a) ε_i and E_F; (b) n_i (solid curves) and d_j ($j=1$, dashed curve and 2, dashed-dotted curve are referred to in Fig. 1) as a function of gate voltage for an $Al_{0.25}Ga_{0.75}As$-GaAs-$Al_{0.25}Ga_{0.75}As$ SQW. N_j, s_j, and N_a are the same as in Fig. 2.

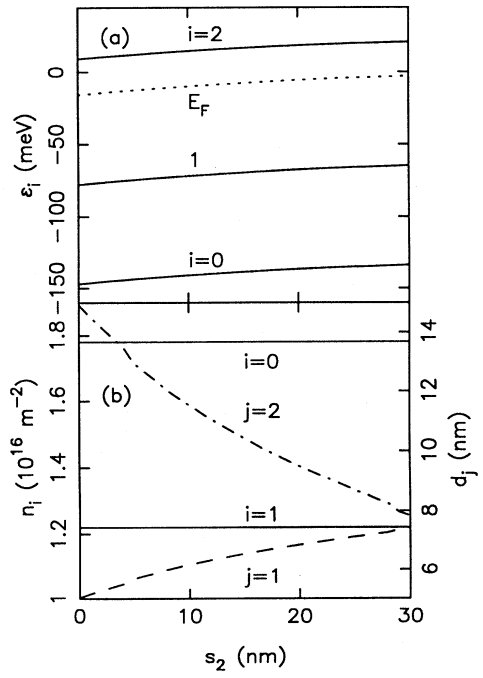

FIG. 9. Influence of asymmetric modulation doping on electronic properties of an $Al_{0.25}Ga_{0.75}As$-GaAs-$Al_{0.25}Ga_{0.75}As$ SQW at $V_g=0$. In the calculation, we take $L=12$ nm, $s_1=5$ nm, $N_1=3\times10^{24}$ m^{-3}, $N_2=10^{24}$ m^{-3}, $N_a=8\times10^{20}$ m^{-3}, $T=4.2$ K, and the parallel magnetic field $B=9$ T. The curves are marked the same as in Fig. 8. s_2 is the spacer distance in the lower $Al_xGa_{1-x}As$ layer in Fig. 1.

The variation of the depletion length results in different distributions of the ionized impurities in the $Al_xGa_{1-x}As$ layers. The result of d_j obtained from the self-consistent calculation would be helpful to the further calculation of the magnetoresistivity (or mobility) caused by impurity scattering, the limiting factor to determine electron transport properties in low temperatures. For a modulation-doped $Al_xGa_{1-x}As$-GaAs-$Al_yGa_{1-y}As$ SQW depicted in Fig. 1, we can model the impurity distribution as

$$n_i(z)=\begin{cases} N_1, & -d_1-s_1-L/2<z<-s_1-L/2 \\ N_a, & -s_1-L/2<z<L/2+s_2 \\ N_2, & L/2+s_2<z<L/2+s_2+d_2\ . \end{cases} \tag{21}$$

Thus, we can calculate the low-temperature magnetoresistivity (or mobility) by taking the known material properties, the sample growth parameters, and the experimental conditions.

IV. SUMMARY AND CONCLUSIONS

In this paper, we studied the electronic structure of two-dimensional electron gas subjected to in-plane magnetic fields. A self-consistent calculation for selectively doped $Al_xGa_{1-x}As$-GaAs-$Al_yGa_{1-y}As$ single quantum wells was developed in which the electronic properties of interest can be calculated as a function of known material properties, sample growth parameters, and experimental conditions. The dependence of the energy level and the electron density in different electronic states, the Fermi energy, and the depletion lengths on the in-plane magnetic field, electron wave vector, Al content, temperature, total electron density, gate voltage, and asymmetric modulation doping was studied in detail. We also discussed the experiment to determine the total electron density in a 2DES in the presence of the parallel magnetic field. Our conclusions are summarized as follows.

A two-dimensional electron system subjected to an in-plane magnetic field provides a quasi-one-dimensional energy structure and an extra parabolic type of confinement potential energy along the z direction.

In the presence of the parallel magnetic field B_x, the Hall configuration in which an additional perpendicular magnetic field B_z is applied can still be used to measure the total electron density of the 2DES. For the case of $B_x^2 \gg B_z^2$ and for a high mobility sample so that $(B_x\mu)^2 \gg 1$, the total electron density per unit area of a 2DES subjected to an in-plane magnetic field can be obtained from measuring the magnetoresistivities ρ_{xx} and ρ_{xy} [see Eq. (20)].

For a selectively doped $Al_xGa_{1-x}As$-GaAs-$Al_yGa_{1-y}As$ SQW, the electronic properties, such as (1) the total confinement potential energy, (2) the energy and wave function of electronic energy levels, (3) the Fermi energy, (4) the electron distribution along the direction perpendicular to the interfaces of SQW, (5) the electron density in different energy levels, and (6) the depletion length in different $Al_xGa_{1-x}As$ layers, can be calculated self-consistently as a function of (1) known material prop-

erties such as effective electron mass and dielectric constant for GaAs, (2) sample growth parameters such as concentrations of doped acceptors and donors, spacer distances, width of the well layer, and Al content, and (3) experimental conditions such as in-plane magnetic field, temperature, and gate voltage. In the calculation, the results for the total electron density and electron wave vector are taken as input parameters.

For a SQW structure, our numerical results show that the experimentally measurable properties such as the electron density and the electronic subband energy measured from the Fermi level depend very little on the quantum number k_y. This implies that k_y may be taken as a quasifree parameter to simplify the self-consistent calculations.

With increasing parallel magnetic field, Fermi energy decreases and leads to the depopulation of electrons in the higher index energy levels. The quantum resonance occurs each time when E_F passes through an energy level. Experimentally, this quantum resonance can be observed from measuring ρ_{xx} versus B_x in low temperatures.

For $Al_xGa_{1-x}As$-GaAs-$Al_yGa_{1-y}As$ SQW systems, the stronger effect of the parallel magnetic field can be observed for the samples with smaller Al content, which results in the comparable confinement potential energies caused by the magnetic field and by the conduction-band discontinuity. The electron density in the occupied levels depends very little on the temperature up to 300 K.

Increasing total electron density will lead to the occupation of electrons to the higher levels and to the rapid increase in depletion lengths. Varying the gate voltage gives rise to (1) the oscillation of the energy levels; (2) the various depletion lengths in the $Al_xGa_{1-x}As$ layers; and (3) the occupation of electrons to the higher levels for a large enough $|V_g|$. The asymmetric modulation doping in a SQW does not affect the electron density in the occupied levels but affects markedly the depletion lengths, which connect to the distribution of the ionized impurities.

ACKNOWLEDGMENTS

This research has been carried out on behalf of the Harry Triguboff AM Research Syndicate. Discussions with Dr. M. P. Das and Dr. C. Jagadish are gratefully acknowledged. The author is grateful to Professor P. Vasilopoulos (Concordia University, Canada) for his useful suggestions and helpful discussions.

[1]F. Stern and W. E. Howard, Phys. Rev. **163**, 816 (1967); F. F. Fang and P. J. Stiles, *ibid.* **174**, 823 (1968); T. Ando, A. B. Fowler, and F. Stern, Rev. Mod. Phys. **54**, 553 (1982).

[2]G. Marx and R. Kümmel, J. Phys. Condens. Matter **3**, 8237 (1991); G. Marx, B. Huckestein, and R. Kümmel, *ibid.* **3**, 6425 (1991); B. Huckestein and R. Kümmel, Phys. Rev. B **38**, 8215 (1988).

[3]D. R. Leadley, R. J. Nicholas, J. J. Harris, and C. T. Foxon, in *Physics of Semiconductors,* edited by E. M. Anastassakis and J. D. Joannopoulos (World Scientific, Singapore, 1990), p. 1609; O. Kühn and P. E. Selbmann, Semicond. Sci. Technol. **6**, 1181 (1991).

[4]J. H. Oh, K. J. Chang, G. Ihm, and S. J. Lee, Phys. Rev. B **48**, 15 441 (1993); S. J. Lee, M. J. Park, G. Ihm, M. L. Falk, S. K. Noh, T. W. Kim, and B. D. Choe, Physica B **184**, 318 (1993).

[5]P. W. Barmby, J. L. Dunn, and C. A. Bates, J. Phys. Condens. Matter **6**, 751 (1994); M. B. Stanaway, C. J. G. M. Langerak, R. A. J. Thomeer, J. M. Chamberlain, J. Singleton, M. Henini, O.H. Hughes, A. J. Page, and G. Hill, Semicond. Sci. Technol. **6**, 208 (1991).

[6]R. J. Nicholas, R. J. Haug, and K. v. Klitzing, Phys. Rev. B **37**, 1294.

[7]T. W. Kim, Y. Kim, M. S. Kim, E. K. Kim, and S.-K. Min, Solid State Commun. **84**, 1133 (1992).

[8]E. Johnson, A. Makinnon, and C. J. Goebel, J. Phys. C **20**, L521 (1987); E. Johnson and A. Makinnon, *ibid.* **21**, 3091 (1988).

[9]F. Piazza, L. Pavesi, H. Cruz, M. Micovic, and C. Mendoca, Phys. Rev. B **47**, 4644 (1993).

[10]A. Elci and D. Depatie, Semicond. Sci. Technol. **9**, 163 (1994).

[11]J. M. Heisz and E. Zaremba, Semicond. Sci. Technol. **8**, 575 (1993).

[12]T. Jungwirth and L. Smrcka, J. Phys. Condens. Matter **5**, L217 (1993).

[13]R. Fletcher, E. Zaremba, M. D'Iorio, C. T. Foxon, and J. J. Harris, Phys. Rev. B **41**, 10 649 (1990).

[14]K. Inoue and T. Matsuno, Phys. Rev. B **47**, 3771 (1993); W. Xu and J. Mahanty, J. Phys. Condens. Matter **6**, 4745 (1994).

[15]T. Jungwirth and L. Smrcka, Superlatt. Microstruct. **13**, 499 (1993).

[16]T. Ando, J. Phys. Soc. Jpn. **51**, 3893 (1982); **51**, 3900 (1982); F. Stern and S. Das Sarma, Phys. Rev. B **30**, 840 (1984); G. A. M. Hurkx and W. van Haeringen, J. Phys. C **18**, 5617 (1985).

[17]C. D. Simserides and G. P. Triberis, J. Phys. Condens. Matter **5**, 6437 (1993).

[18]N. M. Cho, S. B. Ogale, and A. Madhukar, Phys. Rev. B **36**, 6472 (1987); K. Makiyama, K. Kasai, T. Ohori, and J. Komeno, Semicond. Sci. Technol. **7**, B248 (1992).

[19]H. J. Lee, L. Y. Juvrael, J. C. Wolley, and A. J. Spring Thorpe, Phys. Rev. B **21**, 659 (1980).

[20]A. Isihara, Z. Phys. B **73**, 15 (1988); Y. Shiwa and A. Isihara, Phys. Rev. B **27**, 4743 (1983).

[21]Changhong Zhu, Phys. Rev. Lett. **71**, 2288 (1993).

[22]D. G. Kanhere, P. V. Panat, A. K. Rajagopal, and J. Callaway, Phys. Rev. A **33**, 490 (1986).

[23]L. Hedin and B. I. Lundqvist, J. Phys. C **4**, 2064 (1971).

[24]S. E. Koonin and D. Meredith, *Computational Physics* (Addison-Wesley, Reading, MA, 1989).

[25]See, e.g., K. Seeger, *Semiconductor Physics—An Introduction* (Springer-Verlag, Berlin, 1982).